JOURNAL OF VIROLOGY, May 1997, p. 3864–3871 Vol. 71, No. 5
0022-538X/97/$04.00+0

Sequential Action of Six Virus-Encoded DNA-Packaging RNAs during Phage ϕ29 Genomic DNA Translocation

CHAOPING CHEN AND PEIXUAN GUO*

Cancer Research Center, Purdue University, West Lafayette, Indiana 47907

Received 13 December 1996/Accepted 7 February 1997

A 120-base pRNA encoded by bacteriophage ϕ29 has a novel and essential role in genomic DNA packaging. Six DNA-packaging RNAs (pRNAs) were bound to the sixfold symmetrical portal vertex of procapsids during the DNA translocation process and left the procapsid after the DNA-packaging reaction was completed, suggesting that the pRNA participated in the translocation of genomic DNA into procapsids. To further investigate the mechanism of DNA packaging, it is crucial to determine whether these six pRNA molecules work as an integrated entity or each pRNA acts as a functional individual. If pRNAs work individually, then do they work in sequence with communication or in random order without interaction? Results from compensation and complementation analysis did not support the integrated model. Computation of the probability of combination between wild-type and mutant pRNAs and experimental data of competitive inhibition excluded the random model while favoring the proposal that the six pRNAs functioned sequentially. Sequential action of the pRNA also explains why the pRNA is so sensitive to mutation, since the effect of a pRNA mutation will be amplified by 6 orders of magnitude after six consecutive steps, resulting in the observed complete loss of DNA-packaging activity caused by small alterations. When any one of the six pRNAs was replaced with an inactive one, complete blockage of DNA packaging resulted, strongly supporting the speculation that individual pRNAs, presumably together with other components such as the packaging ATPase gp16, take turns mediating successive steps of packaging. Although the data provided here could not exclude the integrated model completely, there is no evidence so far to argue against the model of sequential action.

The double-stranded DNA bacteriophages package their genomic DNAs into a procapsid through a DNA-translocating vertex (portal vertex or connector) with a sixfold symmetry. Packaging of bacteriophage ϕ29 DNA requires the DNA-packaging ATPase gp16 and a virus-encoded 120-base RNA (DNA-packaging RNA [pRNA]), both of which are not a part of the mature virion (14). We have been able to assemble in vitro infectious virions of ϕ29 with all essential components produced from cloned genes or synthesized in vitro (16, 17, 28, 29). The system producing 10^8 PFU per ml of infectious virions without background provides a convenient assay for the function of packaging components (28–30).

Extensive mutagenesis studies of pRNA have shown that pRNA contains at least two functional domains: one responsible for portal vertex binding, and the other responsible for a yet to be defined role in DNA translocation (10, 35, 42, 48, 49, 51). Some mutant pRNAs, with mutations clustering at the 5′-3′ paired ends, retain full procapsid binding affinity but lose DNA-packaging activity completely or partially. Additionally, the binding of pRNA to procapsids has been shown to be an irreversible process for up to 1 h in the presence of Mg^{2+} (35, 41), and the binding is stable upon dilution or ultracentrifugation (41). Many interesting questions remain to be answered. For example, is the pRNA needed only for initiation of DNA packaging, or does it participate in the DNA translocation process? When does the pRNA leave the procapsid? The answers to these questions might help in the elucidation of the biochemical role of the pRNA.

The DNA-translocating portal vertex of ϕ29 is composed of 12 (4, 45), or 13 when assembled from cloned gene products (9, 43), copies of the portal protein, as determined by electron microscopy. Six copies of pRNA (35, 41, 42, 46) attach to each procapsid at the portal vertex (13). In addition to the pRNA, multiple copies of the DNA-packaging ATPase, gp16, are needed to package one genomic DNA (16). Evidence for the binding of gp16 to pRNA-procapsid complexes has also been documented (12, 17, 18). Such observations indicate that the DNA-packaging machinery of ϕ29 is a complex, with multiple copies of each component incorporated, with the DNA-packaging process being accomplished by a collective effort. This collective effort not only means the assemblage of portal vertex, gp16, and pRNA but also means the collective action of each subunit of individual components. To further investigate the mechanism of DNA packaging, it is crucial to determine whether the DNA-packaging machine is an integrated entirety and should be studied as an intact assemblage or whether it can be dissected into the action of individual molecule. If they work individually, then the other question to be answer is whether they work sequentially or in a random style. In other words, can each molecule, e.g., each pRNA, of the multicopy machine take turns to accomplish a single reaction by itself in a chain transmission?

We report in this paper that pRNA was associated with the procapsid during the DNA translocation process and left the procapsid after the DNA-packaging reaction was completed. Our data suggest that the six pRNAs per procapsid that are required for DNA packaging acted consecutively. Breaking of any one of the individual links would result in the termination of the entire process.

An attractive model concerning the mechanism of DNA packaging was proposed by Hendrix in 1978 (21); however, no one has been able to provide direct evidence to support this model. In this model, the fivefold (procapsid shell) and sixfold (portal vertex) symmetry mismatch allows rotation of the portal vertex to provide a driving force for DNA translocation.

* Corresponding author. Mailing address: Hansen Life Sciences Research Building, Cancer Research Center, Purdue University, West Lafayette, IN 47907. Phone: (765) 494-7561. Fax: (765) 496-1795. E-mail: guo@vet.purdue.edu.

The finding that six copies of pRNA are needed for DNA packaging and are bound to the portal vertex is most likely relevant to this proposed symmetry mismatch. The sequential action of pRNA reported here also favors the mechanism proposed in the symmetry mismatch model. It has been shown that approximately one ATP is needed for the packaging of 2 bp of DNA (18), and pRNA causes a fourfold increase in the ATPase activity of the packaging ATPase gp16 (12), suggesting that the pRNA may play a role in the energetics of DNA translocation process. If pRNA serves as part of the molecular pump or mediates the turning of the DNA-translocating motor, then conformational changes of the pRNA could be critical factors in the consideration of transferring chemical energy from ATP into mechanical motion. Indeed, we have found anomalous conformations of the pRNA in variable environments and conditions (reference 7 and unpublished data).

MATERIALS AND METHODS

In vitro ϕ29 assembly. The purification of procapsids (15), gp16 (16), DNA-gp3 (28), and gp9 (29), the synthesis of pRNA (48, 52), and pRNA secondary structure prediction (53), as well as in vitro ϕ29 assembly (29, 30), were performed as described previously.

ϕ29 DNA packaging assay. DNA packaging was performed as described previously (16, 19, 29) except in the presence of either ^{3}H-DNA-gp3 or ^{3}H-pRNA. After DNA packaging, the reaction mixtures were diluted to 100 μl with TMS buffer (50 mM Tris-HCl, 100 mM NaCl, 10 mM $MgCl_2$ [pH 7.8]). The packaging reaction mixtures were loaded directly on to the top of a 5 to 20% sucrose gradient in TMS buffer. The samples were centrifuged in a Beckman L-80 Ultracentrifuge for 35 min at 35,000 rpm in an SW55 rotor. Tail protein gp9 (10 μl) was added to DNA packaging reactions as indicated.

Detection of procapsid-pRNA interactions by filter binding. Filter binding assays were performed as described previously (8, 13, 39, 41). Briefly, purified procapsids (15, 19) were dialyzed on a 0.025-μm-pore-size type VS filter membrane (Millipore Corp.) against TBE buffer (89 mM Tris-borate, 2 mM EDTA [pH 8.0]) for 10 min at 25°C. ^{3}H-pRNA synthesized in vitro with T7 RNA polymerase in the presence of [^{3}H]UTP (10 mCi/ml; Amersham) was mixed with procapsids and dialyzed for another 15 min against TBE. For competition assay, a constant amount of ^{3}H-labeled pRNA was mixed with unlabeled pRNAs in various ratios before being added to procapsids. The procapsid-pRNA mixtures were then dialyzed against TMS buffer for 30 min at 25°C. The mixtures were diluted to 100 μl with TMS and were loaded onto a Whatman 2.4-cm GF/B glass microfiber filter prewetted with TMS. The filter was washed eight times with 1 ml of TMS, dried, and subjected to scintillation counting.

Compensation and complementation studies with pRNAs having mutations at different sites. Mutant pRNAs (Table 1) were constructed as described previously (49–52). To test whether the mutant locus of a pRNA can be rescued by wild-type or other mutant pRNAs, each mutant pRNA was mixed with an equal amount, except otherwise indicated, of wild-type or another mutant pRNA. The activity of each mixture in DNA packaging was assayed with the in vitro ϕ29 assembly system (28–30).

Equations to predict titration curves representing three models. Mutant pRNAs, with binding affinities similar to that of wild-type pRNA, were used to compete with wild-type pRNA for assembly in vitro, as reported previously (28–30, 41). Phage assembly was determined and expressed as PFU/milliliter.

Based on the fact that mutant pRNAs have the same procapsid binding affinity as wild-type phenotype pRNA, a computation was performed to determine the theoretical probability of each procapsid containing a certain number of wild-type and a certain number of mutant pRNAs under certain conditions. The following binomial (41) was used: $(p+q)^z = \binom{z}{0} p^z + \binom{z}{1} p^{(z-1)} q + \binom{z}{1} p^{(z-2)} q^2 + \ldots + \binom{z}{z-1} pq^{(z-1)} + \binom{z}{z} q^z = \sum_{M=0}^{z} \binom{Z}{M} p^{(z-M)} q^M$ (equal to 1), where $\binom{Z}{M}$ is equal to $\left(\frac{Z!}{M!(Z-M)!}\right)$, p and q were the percentages of wild-type and mutant pRNAs, respectively, present in a given mixture, and $p + q = 1$. Z was the total number of pRNA molecules bound to one procapsid. Here $Z = 6$ as determined previously (35, 41, 42, 46). M and N represent the number of mutant and wild-type (or mutant and the other mutant) pRNAs, respectively, bound to an individual procapsid, and $M + N = Z = 6$.

When mutant and wild-type pRNAs were mixed in defined ratios, the probability of procapsids that carried various numbers of wild-type and mutant pRNAs could be calculated. For example, if a mixture consists of 90% wild-type RNA ($p = 0.9$) and 10% mutant ($q = 0.1$) pRNA, the percentage of procapsids carrying two mutant and four wild-type pRNAs was $\frac{6!}{2!\,4!}\, p^4 q^2 = 15\,(0.9)^4\,(0.1)^2 = 9.84\%$. Excess amounts of pRNA were added to each reaction. Here only those procapsids that carried a total of six pRNAs, either mutant or wild type, were considered, since six pRNAs are required for DNA packaging to occur, and any procapsid that carried fewer than six copies of pRNA were not active and could be ignored when PFU/milliliter was considered.

Three models, integrated, sequential individual, and random individual, were proposed to interpret the mechanism of pRNA action (see Results and Discussion for explanation).

The models were tested by using inhibition of ϕ29 assembly with partially active mutant pRNAs (i.e., mutant pRNAs that produce a reduced PFU/milliliter yield when used in in vitro assembly assays). Given that Y and X were the yields of infectious ϕ29 assembled, expressed as PFU/milliliter, when 100% wild-type and 100% mutant pRNAs, respectively, were used, and D is a reduction factor which equals $\frac{Y}{X}$, then $X = \frac{Y}{D}$. In a reaction mixture containing both mutant and wild-type pRNAs in a given ratio, the probability of active procapsids carrying only wild-type pRNA (six copies) is p^6. The infectious phage produced by these procapsids would be Yp^6 PFU/ml. Similarly, the probability of procapsids carrying only mutant pRNA (six copies) is q^6. The infectious phage produced by these procapsids would be $Xq^6 = \frac{Y}{D} q^6$. The PFU/milliliter yield from these two classes of procapsids is a function of the ratio of wild-type to mutant pRNA in the reaction, regardless of which model was adopted. However, for those procapsids that possess both wild-type and mutant pRNAs, the expected yields are different depending on which model is considered. With the integrated model, the yield was predicted by $[Y(1 - q^6) + \frac{Y}{D} q^6]$, since only those procapsids carrying six copies of mutant pRNA could have reduced activity. For the random individual model, the yield (PFU/milliliter) for procapsids possessing both wild-type and mutant pRNAs was predicted with the equation $Y \frac{1}{D} \binom{Z}{M} p^{(Z-M)} q^M$ ($M = 1, 2, \ldots 5$). For the sequential individual model, the yield was predicted with the equation $Y \left(\frac{1}{\sqrt[3]{D}}\right)^{(M)} \binom{Z}{M} p^{(Z-M)} q^M$ ($M = 1, 2, \ldots 5$). The sum of the PFU/milliliter yields for procapsids with only wild-type, only mutant, and combinations of both wild-type and mutant pRNAs bound would be the predicted total yield.

RESULTS

pRNA remained associated with DNA-filled capsids. It is known that pRNA is absolutely required for DNA packaging, though it does not exist in mature virions. One of the questions that has not been answered is whether the pRNA is needed only for the initiation of DNA packaging or whether it participates throughout the DNA translocation process. To address this question, ^{3}H-pRNA was used to package unlabeled DNA-gp3 in vitro. It was found that ^{3}H-pRNA was present in the radioactive peak corresponding to the location of DNA-filled capsids in sucrose gradients (Fig. 1), suggesting that the pRNA is associated with the DNA packaging machinery during the DNA translocation process under the conditions of this in vitro reaction.

pRNA leaves DNA-filled capsid after the addition of the tail protein gp9. It is known that the pRNA is not present in the mature virion but is required for DNA packaging. It is not known when the pRNA leaves the procapsid. To address this concern, sucrose gradient sedimentation was used to detect assembly intermediates. It was found that in the presence of the tail protein gp9, via the addition of gp9 before or after DNA packaging, the pRNA was no longer associated with the DNA-filled capsid (Fig. 2). The result suggests that gp9 can cause the release of pRNA from DNA-filled capsids. However, gp9 did not cause the release of pRNA from DNA-free procapsids, since after the addition of gp9 the ^{3}H-pRNA peak corresponding to the location of pRNA-procapsid complexes did not decrease (Fig. 2).

pRNAs used in competition study had similar procapsid binding affinities. As mentioned above, some mutant pRNAs with procapsid binding affinities similar to that of wild-type pRNA showed reduced phage yield when used in in vitro ϕ29 assembly assays. To compare the procapsid binding affinities of mutant pRNAs used in this study, binding competition experiments were performed. ^{3}H-labeled wild-type phenotype pRNA 7/11 was incubated with procapsids in the presence of various amounts of unlabeled pRNA 7/11 or other mutant pRNAs. Mutant pRNAs 26b/d114 and 26a/27 (51) showed procapsid

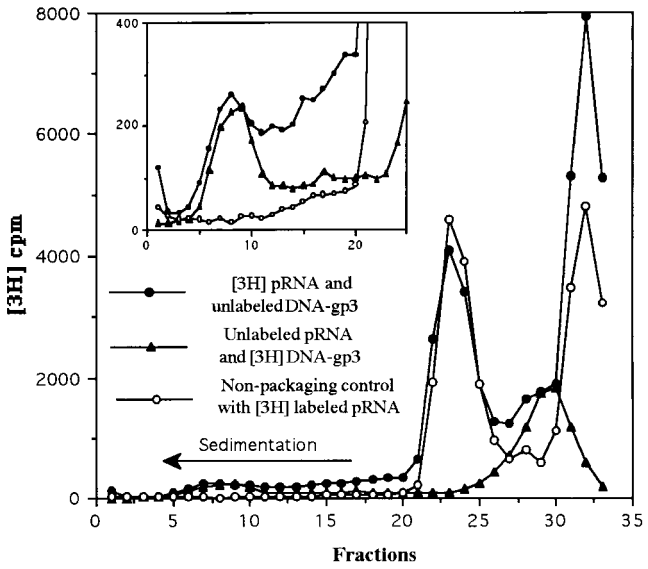

FIG. 1. Profile of sucrose gradient sedimentation showing the association of pRNA with DNA-filled capsids. DNA-gp3 packaging was performed with unlabeled components with the exception of either ^{3}H-pRNA (solid circles) or ^{3}H-DNA-gp3 (triangles). The pRNA-procapsid complexes were centered at fraction 23, and DNA-filled capsids were centered at fraction 8. An enlarged plot (inset) shows that ^{3}H-pRNA was present at the same location in the gradient as the complex containing ^{3}H-DNA-gp3.

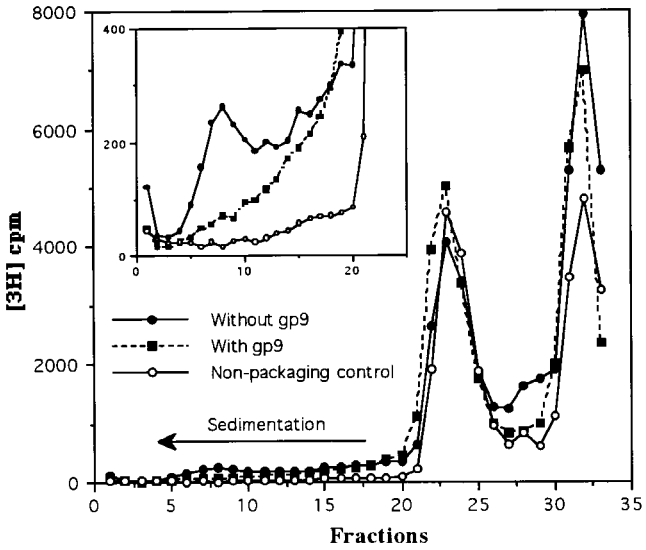

FIG. 2. Profile of sucrose gradient sedimentation showing the dissociation of pRNA from DNA-filled capsids after the addition of the tail protein gp9. DNA-gp3 packaging was performed with ^{3}H-pRNA and unlabeled DNA-gp3. The pRNA-procapsid complexes were centered at fraction 23, and DNA-filled capsids were centered at fraction 8. In the absence of gp9 (solid circles), ^{3}H-pRNA was detected in the peak representing the DNA-filled capsids. However, after the addition of gp9 (squares), ^{3}H-pRNA was no longer detected in the peak representing DNA-filled capsids, as shown in the inset.

binding affinities that were indistinguishable from that of wild-type phenotype pRNA 7/11 (Fig. 3). Thus, mutant and wild-type pRNAs should be able to compete equally for procapsid binding sites when mixed together. Recent studies on pRNA-procapsid binding indicate that the binding of both mutant and wild-type pRNA is irreversible for the time periods being studied in this work (35, 41).

Three proposed models for pRNA action. It has been reported that each procapsid contained six copies of pRNA (13, 35, 41, 46). To further the investigation of the mechanism of DNA packaging, it is crucial to determine whether the DNA-packaging machine is an entirety and should be studied as an intact assemblage (an integrated model) or whether it can be dissected into the functions of each individual molecule. If six pRNA molecules works individually, then do six pRNAs work consecutively (sequential individual model), or does each pRNA contribute one step of each reaction cycle consisting of six steps but in random order (random individual model)? We propose these three models to distinguish these possibilities. The distinction among these three models can be illustrated by analogy inference to three intelligence competitions, each with different scoring rules. In this example, each team has six members. In the integrated game style, a question is presented to the team and answered after discussion by collaboration or by any one of the members who knows the correct answer. When the correct answer is given, the team receives a positive score. The sequential individual game style requires each member to answer a question in sequence. A failure to answer the question by any one of the members could result in the appearance of the notice "Game Over." The total score in this case will be the sum of the scores of the successive members who have provided acceptable answers. In the random individual game style, the question is answered by all six members in no specific order; if any team member provides an incorrect answer, the whole team is wrong. In the integrated game style, the total team score is not affected by the number of nonintellectual members on the team, as long as the team contains one very intelligent member, whereas in both individual styles (sequential and random), the total team score is affected by the number of nonintellectual members on the team. The rules concerning these three game styles could also explain the motive to design compensation and complementation analyses to distinguish the models (see below). In the integrated style, the deficiency of any nonintellectual team member(s) could be compensated for by a very intelligent member; however, in the individual game styles, such a deficiency cannot be compensated for due to the participation of all members. Regarding the packaging system, consider a mutant pRNA molecule with a 10-fold reduction in its activity compared to wild-type pRNA. If pRNA works integrally, only those procapsids carrying six copies of mutant pRNA are considered to have 10% of the activity, since the compensation by wild-type pRNA will confer full activity to the procapsids carrying one, two, three, four, or five mutants. However, if the pRNA acts consecutively, those procapsids carrying one partially active pRNA and five wild-type pRNAs will produce a 10-fold reduction in in vitro DNA packaging, those carrying two partially active pRNAs and four wild-type pRNAs will produce a $10 \times 10 = 100$-fold reduction, and so forth. Finally, those procapsids carrying six partially active pRNAs will produce a $10 \times 10 \times 10 \times 10 \times 10 \times 10 = 10^6$-fold reduction in in vitro DNA packaging. If the pRNA works randomly, a 10-fold reduction in PFU/milliliter would result regardless of how many copies of partially active pRNA are incorporated into one procapsid. This is because the lowest score of the member on the team is taken as a team score according to the rule of this game style. Accordingly, the inhibition effect will be more profound with the individual models than with the integrated model.

Competition assay of phage assembly suggested that six pRNA molecules worked sequentially. To test which model matches our experimental data, partially active pRNAs were mixed with wild-type phenotype pRNA in various molar ratios

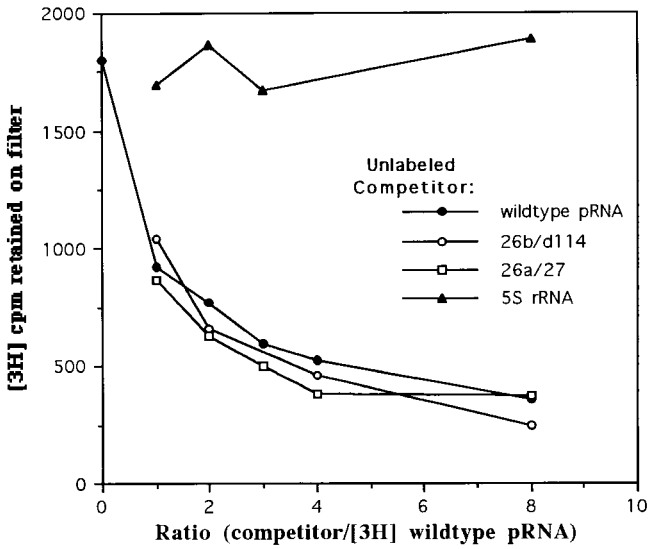

FIG. 3. Competitive binding assay to compare the procapsid binding affinities of partially active mutant pRNAs. Various ratios of ^{3}H-labeled pRNA 7/11 (wild-type phenotype) to unlabeled competitor pRNA were mixed with a fixed amount of procapsid and assayed by filter binding (8, 13, 39). Unlabeled pRNA 7/11 and 5S rRNA served as positive and negative controls, respectively.

and assayed for their activities in in vitro ϕ29 assembly. Two partially active pRNAs, 26b/d114 and 26a/27, were used. The procapsid binding affinities of these two mutants were indistinguishable from that of wild-type pRNA (Fig. 3). Mutant pRNAs which allowed no plaque production when used in in vitro assembly were not used in this experiment for several reasons: (i) the failure in complementation with two inactive pRNAs (see below and Table 1) excluded the integrated model; (ii) our previous work showing that DNA packaging can be completely blocked by binding of only one inactive pRNA to an otherwise wild-type-saturated procapsid has already favored the sequential model (42); and (iii) a reduction factor in activity cannot be calculated when the yield of infectious virus (PFU/milliliter) with 100% mutant pRNA is zero.

The empirical plot of yield of in vitro phage assembly versus percent mutant pRNA was then compared with predicted plots. In this experiment, the activity of the partially active mutant pRNA 26b/d114 was 3.4×10^3, as determined by PFU/milliliter yield in in vitro assembly reactions in the absence of wild-type pRNA, while the activity of wild-type pRNA alone in packaging reactions was 2.3×10^7. Therefore, the activity of pRNA 26b/d114 was reduced $(2.3 \times 10^7)/(3.4 \times 10^3) = 6{,}765$-fold. With the integrated model, the yield was predicted by $[Y(1 - q^6) + \frac{Y}{D}q^6]$, since only those procapsids catching six copies of mutant would produce reduced yield; the rest of the procapsids would be as active as all wild-type procapsids. If nonsequential (random individual models) was applied, the 6,765-fold reduction in activity could be caused by a single pRNA 26b/d114 per procapsid, and incorporation of two, three, four, five, or six copies of pRNA 26b/d114 would make no difference. Therefore, the PFU/milliliter was predicted with the sum of $Y\frac{1}{D}\binom{Z}{M}p^{(Z-M)}q^M$, Yp^6, and $\frac{Y}{D}q^6$ (see Materials and Methods), where Y was PFU/milliliter produced when 100% wild-type pRNA was used for packaging reaction and D represented the reduction factor of activity when 100% mutant pRNA was used (here, $D = 6{,}765$).

If the sequential individual model is applied, 6,765-fold reduction was contributed by $Z = 6$ copies of pRNA per procapsid, and each pRNA would cause a $\sqrt[6]{6{,}765}$-fold reduction. The probability of a certain procapsid catching M copies of pRNA 26b/d114 and $(6 - M)$ copies of wild-type pRNA was predicted as $\binom{Z}{M}p^{(Z-M)}q^M$; thus, the yield was $Y(\frac{1}{\sqrt[6]{D}})^M\binom{Z}{M}p^{(Z-M)}q^M$ $(M = 1, 2, \ldots 5)$. The sum of each item will be the predicted value of PFU/milliliter (Fig. 4b). Comparison of empirical curves and predicted curves indicates that our results agreed with the sequential individual model,

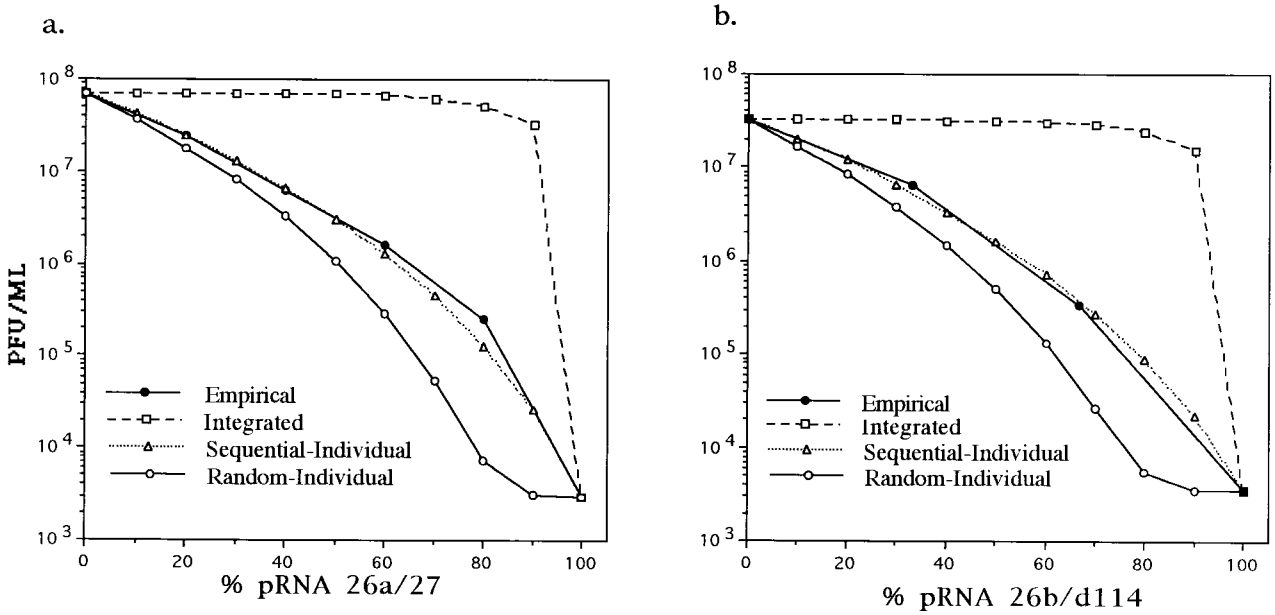

FIG. 4. Comparison of semilog plots of the empirical data with the plots predicted by the computer program Microsoft Excel, with formulas signifying three models of pRNA action. Curves represent the yield of virion production versus percentage (molar ratio of mutant to wild type) of mutant pRNA in the assembly mixture. Wild-type pRNA was mixed with various amounts of mutant pRNA 26A/27 (a) or 26b/d114 (b) and assayed with the in vitro ϕ29 assembly system.

since the empirical curve overlapped the curve predicted with this model. Comparison of the empirical inhibition curve with the predicted curve of another partially active pRNA, 26a/27, produced the same results (Fig. 4a), albeit the activity of pRNA 26a/27 was different from that of pRNA 26b/d114. The essential difference between the two theoretical curves predicted from these two models is the shape and slope of the curve. The match of shape and slope of the empirical curve with the curve predicted with the sequential individual model was reproducible when four other partially active mutant pRNAs were tested in this manner (data not shown).

Complete inactivation of pRNA by one single-base mutation favored the sequential model. We previously showed that in many cases, a single-base mutation of the pRNA resulted in pRNAs that were completely inactive in DNA packaging, as demonstrated by the lack of plaque formation when these mutant pRNAs were used in in vitro assembly (51). Typically, 10^7 plaques per ml can be obtained with wild-type phenotype pRNA. No plaque formation means a more than 10^7-fold reduction in activity. Such a large reduction in activity is quite striking yet can be easily explained by the sequential individual model. For example, given that a one-base mutation resulted in a mutant pRNA with a 20-fold reduction in individual activity, ϕ29 assembly with this mutant pRNA could produce (10^7 PFU/ml $\times$ 1/20) = 5×10^5 PFU/ml, if the mechanism of either the integrated or the random individual model is applied. However, if the mechanism of the sequential individual model is applied, in vitro assembly could produce [10^7 PFU/ml $\times$ $(1/20)^6$] $\cong$ 0 PFU/ml, which is mostly observed with mutagenesis assays (50, 51).

Failure in compensation and complementation tests excluded the integrated model. A compensation test is a way to distinguish the integrated model from two individual models (see "Three proposed models for pRNA action" above). Here the term "compensation test" is different from "complementation test," which means the crossing between two mutants, in that the former covers the implication of whether the wild-type pRNA can compensate for certain defects of mutant pRNA in ϕ29 assembly. One mutant pRNA was mixed with wild-type phenotype pRNA for compensation analysis or with another mutant pRNA for complementation analysis. Our extensive investigation showed that not a single plaque was produced in any complementation test with any two inactive pRNAs with mutations at two different locations (Table 1 and data not shown), except suppressor mutations for inter-pRNA interactions (unpublished data). Moreover, the yield of a complementation test with two partially active pRNAs had never been higher than the yield produced with one of the more active pRNAs alone (data not shown). Mutant pRNAs 26a/27, 8/9 (51), p8/p4 (41, 42), 7/GGU, 108/G99, 14-17/10, 7/100-103, 14-16/10, 26a/27, 26b/d114 (51), cpRNAs 5/31, and 55/54 (Fig. 5) were used for a compensation test with wild-type phenotype pRNA 7/11. Some of these pRNAs, e.g., 108/G99 (50), had a mutation of one base only. The compensation test showed that the wild-type phenotype pRNA could not compensate for the defect of any one of these mutants (Table 1 and data not shown). The failure of wild-type pRNA to compensate for the defect in mutant pRNAs was clearly documented by the results of inhibition assays in which the activity of wild-type pRNA was strongly inhibited by mutant pRNA (41, 42, 50). The failure of wild-type pRNA to compensate for mutant pRNAs and the success of mutant pRNAs in inhibiting wild-type pRNA were also demonstrated by an almost perfect match in comparing the empirical yield with the theoretical yield predicted based on the sequential model (Table 1). This failure in compensation could not be explained by a structural change of the procapsid binding domain of mutant pRNAs, since some of the mutant pRNAs (Fig. 5), e.g., P8/P4 (41), 26a/27, 26b/d114 (51), and 7/GGU (50), had procapsid binding affinities that were equal to that of wild-type pRNA (reference 41 and Fig. 3). Computer folding and chemical probing showed that the structures of the procapsid binding domains of P8/P4 and 7/GGU were identical to that of wild-type pRNA (unpublished data). The failure to compensate supports the speculation that the six pRNAs work sequentially.

The fact that compensation and complementation studies with inactive pRNAs did not work did not exclude the integrated model completely. However, had two separate pRNAs been able to compensate for or complement each other, then it may have been possible to claim that the pRNAs acted as an integrated entirety. As it stands, complementation was not observed with various mutant pRNAs, which tends to not support the integrated model of pRNA function.

Complete blockage of DNA packaging by one inactive pRNA supports sequential action. In vitro ϕ29 assembly in the presence of both mutant and wild-type pRNAs showed that any one of the six pRNAs, if replaced with an inactive one, could block DNA packaging completely (41, 42), which strongly supports the speculation that individual pRNAs take turns mediating successive steps of DNA packaging. The way that one inactive pRNA can result in complete blockage is best explained by sequential action.

TABLE 1. Compensatory and complementary assay of pRNAs with different mutants[a]

RNA	pRNA P8/P4		pRNA 7/GGU		pRNA 26b/d114		cpRNA 5/31	
	Predicted	Empirical	Predicted	Empirical	Predicted	Empirical	Predicted	Empirical
pRNA p8/p4	NA	0	0	0	3.4×10^3	4×10^3	0	0
pRNA 7/GGU	0	0	NA	0	3.4×10^3	4×10^3	0	0
pRNA 26b/d114	3.4×10^3	4×10^3	3.4×10^3	4×10^3	NA	2.3×10^5	ND	ND
cpRNA 5/31	0	0	0	0	ND	ND	NA	0
Wild-type pRNA 7/11	0%, 1.0×10^8	0%, 1.0×10^8	0%, 1.0×10^9	0%, 1.0×10^9	0%, 4×10^7	0%, 4×10^7	ND	ND
	25%, 1.8×10^7	25%, 2.2×10^7	33%, 8.8×10^7	33%, 5.3×10^7	50%, 5.2×10^6	50%, 9×10^6	ND	ND
	50%, 1.6×10^6	50%, 2.4×10^6	67%, 1.4×10^6	67%, 7.0×10^6			ND	ND

[a] Compensation and complementation studies to distinguish the integrated model from two individual models. Values correspond to predicted or empirical yields of in vitro ϕ29 assembly reactions in the presence of pRNAs from both the left column and the top row. For example, the lower left values, of 50% and 1.6×10^6 indicate that the predicted yield of in vitro assembly in the presence of 50% of pRNA P8/P4 and 50% pRNA 7/11 was 1.6×10^6 PFU/ml. The percent indicates the molar ratio of the pRNAs on the top row over the left column. The pRNAs were mixed in equal molar ratios unless otherwise indicated. The theoretical yield (PFU/milliliter) was predicted with the binomial based on the assumption that the six pRNAs work sequentially (see Materials and Methods) and no compensation or complementation could occur. 0, no plaque formation; NA, not applicable; ND, not done; cpRNA, circularly permuted pRNA (50, 52).

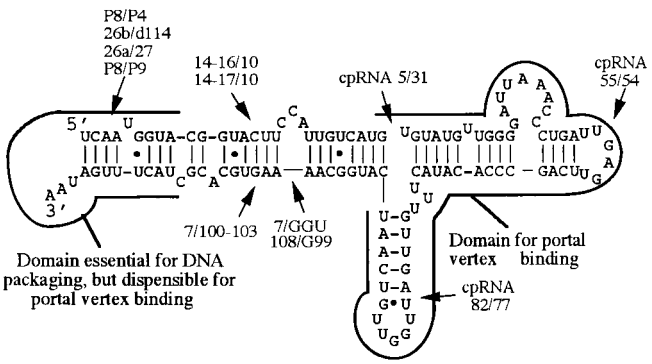

FIG. 5. Secondary structures and functional domains of pRNA. The locations of mutant pRNAs are indicated with arrows. cpRNA, circularly permuted pRNA (50, 52).

DISCUSSION

The following models, integrated, sequential individual, and random individual, were used to interpret the mechanism of pRNA action. Compensation and complementation studies

mechanism of pRNA action < integrated model / individual model < random model / sequential model

did not support the integrated model but favored individual models. Concerning two individual models, competitive inhibition excluded the random individual model. Therefore, the evidence supports the speculation that six pRNA molecules work sequentially.

A common structural feature among the double-stranded DNA phages is that a portal vertex, or connector (26, 32, 36), with 12 (1–6, 38, 45) or 13 subunits (9, 43) is embedded in an icosahedral protein shell that has a fivefold rotational symmetry. This symmetry mismatch has previously been proposed to play a key role in DNA translocation (21). Rotation of the portal vertex, which has previously been reported as having a sixfold symmetry, in a fivefold symmetric environment could constitute a mechanical motor in which the relative motion of the two rings could drive the DNA into the procapsid. Although the idea of the generation of physical force from a rotary motor with a symmetry mismatch between two rings is particularly interesting, no one has been able to prove this model directly with experimental data. Since six copies of pRNA are attached to the portal vertex and each is needed for DNA translocation, how could our data be used to interpret the symmetry mismatch model mentioned here? First, let us consider sequential action of pRNA. Other than the two rotational rings, at least one additional component is needed to turn the ring. The DNA-packaging enzyme gp16 or pRNA could be the candidate for this third component. Analogous to the four or six cylinders in the engine of a car, sequential action is a way to turn the motor (Fig. 6). By "sequential," it is meant that multiple pRNAs (again, in conjunction with other components) involved in DNA packaging appear to act such that a step-by-step process is performed, with each pRNA exerting its effect alternatively (Fig. 6). Therefore, sequential action of pRNA favors the symmetry mismatch model of Hendrix (21).

In this work, we provide evidence that the ϕ29 pRNA is associated with procapsids during the DNA translocation process. Our inhibition data also suggest that the pRNA plays an essential role in DNA translocation. How could pRNA perform a physical task in collaboration with other components to force DNA into a protein shell? Obviously, conformational changes in the pRNA are a way to explicate a process involving migration and motion. We have documented a conformational change of pRNA before binding to procapsid (7). More than one conformational change in pRNA is expected during this elaborate and intricate DNA-packaging process. Interaction of pRNA with each participating component, such as the subunits

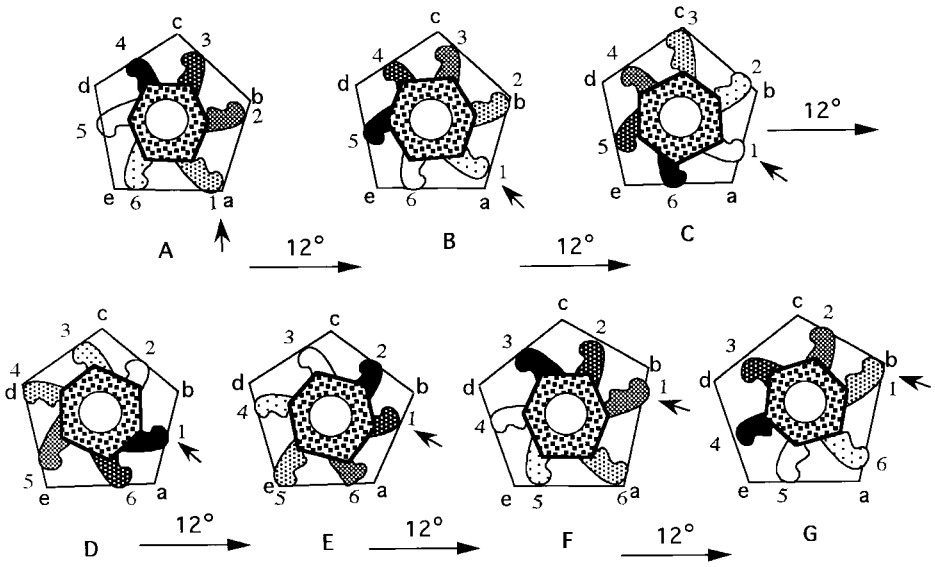

FIG. 6. A model depicting the sequential action of pRNA in ϕ29 DNA packaging. The hexagon represents the connector (portal vertex), and the surrounding pentagon represents the head membrane. Six protrusions represent six pRNAs. The variable shapes and patterns portray the pRNA (alone or with other components) in serial energetic states. Some, such as pRNA 4 in panel A, are in a contracted conformation, and others, such as pRNA 1 in panel A, are in an extended conformation. Arrows point to the different energetic states of pRNA 1. A to G represent six steps of rotation. Each step rotates 12°, since a five- to sixfold symmetry mismatch generates 30 equivalent orientations (360°/30 = 12°). The portal vertex turns 72° after six steps. For example, pRNA 1 moves from vertex a (A) to vertex b (G) and rotates 72°. Each step requires one ATP to initiate one pRNA conformational change, and six ATPs are needed for the transition from one vertex to an other vertex. Therefore, 30 ATPs are needed for one 360° rotation. The drawing is the view from inside the procapsid.

of the portal vertex or the protein shell, might result in conformational changes. These conformational changes, driven by ATP hydrolysis, could result in physical transition to drive the motor.

It is well accepted that the energy to drive DNA packaging is supplied by the hydrolysis of ATP (3, 11, 18, 20, 22, 24, 25, 27, 31, 33, 34, 37, 40). Figure 6 shows a model proposed to explain the relationship between the rotational mismatch and the revolving of the portal vertex. The driving force for the rotation of the portal vertex in this model is a conformational change of the pRNA or a pRNA-gp16 complex. The linkage between a conformational change and the production of a driving force is also depicted. In each of the six steps of the rotational process, the portal vertex turns 12° [360°/(5 × 6)]. The six protrusions from the sixfold symmetrical portal vertex represent six copies of the pRNA or pRNA-gp16 complexes. The protrusion exists in two conformational states, extended and contracted. Contracted conformation allows a favorable interaction with the middle of the sides of the pentagonal protein shell. The extended conformation allows a favorable interaction with one of the five vertices of the pentagon. The transition from the contracted to the extended conformation, derived from ATP hydrolysis (47), could generate a physical force for rotation between the fivefold/sixfold rings. At one given time during DNA packaging, one of the six protrusions is approaching one vertex of pentagon. During rotation, interaction of one protrusion with one specific location of the ring allows ATP hydrolysis to occur. Sequential interaction of the protrusion with the fivefold symmetrical protein shell results in the continuous rotation. From A to G (Fig. 6), each protrusion undergoes one conformational change. For example, pRNA 1 traveled from vertex a to vertex b after six transitions and will turn the portal vertex 72° (360°/5). Thus, six conformational changes of six different protrusions are required to rotate the portal vertex 72°. Each conformational change requires at least 1 ATP, and thus 6 ATPs allow the portal vertex to rotate 72° and 30 ATPs allow the portal vertex to rotate 360°.

Two models for DNA translocation into the procapsid have been proposed previously. One model assumes that the DNA is translocated through the axial hole of the portal vertex, much like a threaded rod moving along a nut (21). The second model hypothesizes that supercoiled DNA wraps around the portal vertex and rotation of the portal vertex allows DNA to pass into the procapsid via the outside of the portal vertex (44), much like a cable wrapping around a roller when pumping water from the well.

If DNA passes through the axial hole of the portal vertex, then six ATPs are needed to package 2 bp of DNA. This number was derived from the consideration that 10.5 bp of B-DNA constitute a helical turn of 360°. The turning of each base pair requires the rotation of 36°, and the turning of 2 bp requires the rotation of 72°. As mentioned above, six ATPs are required to rotate the portal vertex 72°, and thus six ATPs are needed for the packaging of 2 bp. The ATP requirement with this model is sixfold higher than the experimentally measured one ATP per 2 bp of DNA packaged (18).

If DNA passes through the outside of the portal vertex, the energy consumption would be much lower and would compare favorably to the empirical number determined previously in both ϕ29 (0.5 ATP/bp) (18) and T3 (0.55 ATP/bp) (33) in the in vitro systems. Previous studies reported that 180 bp of DNA were wrapped around the outside of the portal vertex (44). As described above, 6 ATPs are required to rotate the portal vertex 72°; that is, 30 ATPs are needed for one complete portal vertex rotation. Thus, 0.17 ATP is needed for the packaging of 1 bp, assuming that 180 bp of DNA wrap around the portal vertex one time (30 ATP/180 bp). Since ATP might be also needed for the initiation of the binding of DNA to procapsid (20) and might be needed for other reactions during the DNA-packaging process, the higher observed energy requirement than predicted from the model is not surprising. On the other hand, when the diameter of the portal vertex is considered, the predicted ATP requirement would compare more favorably to the empirical number of 0.5/bp. The diameter of the portal vertex of ϕ29 is 8 to 14 nm; thus, its circumference is 24 to 52 nm. A DNA fragment with 75 to 162 bp (3.4 nm/10.5 bp) would be able to wrap around the portal vertex once. Therefore, 0.4 to 0.2 ATP would be needed to package 1 bp (30 ATP/(75 − 162) bp), which is fairly close to the experimentally determined 0.5 ATP/bp.

A symmetry mismatch between the portal vertex and the fivefold symmetric phage head exists regardless of whether the portal vertex has 12 or 13 subunits. Dubé et al. (9) have proposed two interesting models for DNA packaging with 12- and 13-fold symmetrical portal vertices. The 12-fold model differs from the 13-fold model when the number of ATPs required to rotate the portal vertex is considered. The model suggests that a unit rotation of 18° consumes one ATP and allows the packaging of 2 bp of DNA. This translates to 20 ATPs per portal vertex rotation, which is less than our prediction of 30 ATPs. However, the interactions of the DNA with a 12-subunit portal vertex are predicted to be sterically less favorable than those with a 13-fold portal vertex. Additionally, DNA packaging by this mechanism excludes the interaction of two-thirds of the 12 portal vertex subunits with the DNA. This model addresses the observation that one ATP is for each 2 bp of DNA packaged. However, for the ϕ29 system, the role of the pRNA was not addressed.

The 13-fold model involves the rotation of the portal vertex and interaction of portal vertex subunits in the order 1-4-7-10-13-3-6-9-12-2-5-8-11-1 with every other base pair of genomic DNA. Rotation of the portal vertex for 11° resulted in the packaging of 2 bp. The 11° rotation consumes one ATP, and thus one ATP is consumed per 2 bp. This model proposes that rotation of the portal vertex involves a 13-subunit portal vertex rotating in a fivefold symmetrical environment. Our model differs in that we propose that a sixfold symmetrical portal vertex (or the complex of portal vertex with pRNA and/or gp16) rotates in the same fivefold symmetrical environment. As mentioned above, our model suggests that 30 ATPs are needed for the portal vertex to rotate 360°. Therefore, one ATP is needed to package 1.8 bp {30 ATP/[(360°/11°) × 2 bp]} if the 13-fold symmetrical portal vertex model is used to interpret our model. This number is quite close to the experimentally determined ATP consumption (18, 20). However, the 13-fold model does not take into consideration the additional symmetry mismatch between the portal vertex and the sixfold symmetrical tail or the six copies of pRNA that are known to bind the portal vertex.

We believe that we have to consider the mechanism of DNA packaging as consisting of two steps. The first step is the rotation of the portal vertex; the second is the translocation of DNA. Regarding portal vertex rotation, we are in favor of Hendrix's five- and sixfold mismatch model, since six pRNAs are needed for DNA packaging and all pRNAs bound to the portal vertex work sequentially. The 13-fold model cannot account for the six copies of pRNA and the sixfold symmetry of the phage tail. However, regarding DNA translocation, we are in favor of the model of Dubé et al., since it is compatible with the number of ATPs consumed as determined experimentally.

Although the data provided here do not completely exclude the possibility that DNA packaging occurs by the integrated

model proposed above, there is no evidence so far to argue against the sequential model.

ACKNOWLEDGMENTS

We thank Dwight Anderson for his review of the proposed model regarding pRNA action, Mark Trottier for critical comments on the manuscript, and Chunlin Zhang for performing complementation tests.

This work was supported by NIH grants GM48159 and GM46490.

REFERENCES

1. **Bazinet, C., and J. King.** 1985. The DNA translocation vertex of dsDNA bacteriophages. Annu. Rev. Microbiol. **39:**109–129.
2. **Bazinet, C., J. Benbasat, J. King, J. Carazo, and J. Carrascosa.** 1988. Purification and organization of the gene 1 protoprotein required for phage P22 DNA packaging. Biochemistry **27:**1849–1856.
3. **Becker, A., and M. Gold.** 1988. Prediction of an ATP reactive center in the small subunit, gpNul of phage lambda terminase enzyme. J. Mol. Biol. **199:**219–222.
4. **Carazo, J. M., L. E. Donate, L. Herranz, J. P. Secilla, and J. L. Carrascosa.** 1986. Three-dimensional reconstruction of the connector of bacteriophage ϕ29 at 1.8 nm resolution. J. Mol. Biol. **192:**853–867.
5. **Casjens, S., and R. Hendrix.** 1988. Control mechanisms in dsDNA bacteriophage assembly, p. 15–92. *In* R. Calendar (ed.), The bacteriophages, vol. 1. Plenum Publishing Corp., New York, N.Y.
6. **Cerritelli, M. E., and F. W. Studier.** 1996. Purification and characterization of T7 head-tail connectors expressed from the cloned gene. J. Mol. Biol. **285:**299–307.
7. **Chen, C., and P. Guo.** 1997. Magnesium-induced conformational change of packaging RNA for procapsid recognition and binding during phage ϕ29 DNA encapsidation. J. Virol. **71:**495–500.
8. **Coombs, D. H., and G. D. Pearson.** 1978. Filter-binding assay for covalent DNA-protein complexes: adenovirus DNA-terminal protein complex. Biochemistry **75:**5291–5295.
9. **Dubé, P., P. Tavares, R. Lurz, and M. van Heel.** 1993. The portal protein of bacteriophage SPP1: a DNA pump with 13-fold symmetry. EMBO J. **12:** 1303–1309.
10. **Garver, K., P. Chipman, T. Baker, and P. Guo.** Minimum pRNA sequence requirement for specific portal protein binding and DNA packaging of phage ϕ29. Unpublished data.
11. **Griess, G. A., P. Serwer, V. Kaushal, and P. M. Horowitz.** 1986. Kinetics of ethidium's intercalation in packaged bacteriophage T7 DNA: effects of DNA packaging density. Biopolymers **25:**1345–1357.
12. **Grimes, S., and D. Anderson.** 1990. RNA dependence of the bacteriophage ϕ29 DNA packaging ATPase. J. Mol. Biol. **215:**559–566.
13. **Guo, P., S. Bailey, J. W. Bodley, and D. Anderson.** 1987. Characterization of the small RNA of the bacteriophage ϕ29 DNA packaging machine. Nucleic Acids Res. **15:**7081–7090.
14. **Guo, P., S. Erickson, and D. Anderson.** 1987. A small viral RNA is required for *in vitro* packaging of bacteriophage ϕ29 DNA. Science **236:**690–694.
15. **Guo, P., S. Erickson, W. Xu, N. Olson, T. S. Baker, and D. Anderson.** 1991. Regulation of the phage ϕ29 prohead shape and size by the portal vertex. Virology **183:**366–373.
16. **Guo, P., S. Grimes, and D. Anderson.** 1986. A defined system for *in vitro* packaging of DNA-gp3 of the *Bacillus subtilis* bacteriophage ϕ29. Proc. Natl. Acad. Sci. USA **83:**3505–3509.
17. **Guo, P., C. Peterson, and D. Anderson.** 1987. Initiation events in *in vitro* packaging of bacteriophage ϕ29 DNA-gp3. J. Mol. Biol. **197:**219–228.
18. **Guo, P., C. Peterson, and D. Anderson.** 1987. Prohead and DNA-gp3-dependent ATPase activity of the DNA packaging protein gp16 of bacteriophage ϕ29. J. Mol. Biol. **197:**229–236.
19. **Guo, P., B. Rajogopal, D. Anderson, S. Erickson, and C.-S. Lee.** 1991. sRNA of bacteriophage ϕ29 of *B. subtilis* mediates DNA packaging of ϕ29 proheads assembled in *E. coli*. Virology **185:**395–400.
20. **Hamada, K., H. Fujisawa, and T. Minagawa.** 1987. Characterization of ATPase activity of a defined *in vitro* system for packaging of bacteriophage T3 DNA. Virology **159:**244–249.
21. **Hendrix, R. W.** 1978. Symmetry mismatch and DNA packaging in large bacteriophages. Proc. Natl. Acad. Sci. USA **75:**4779–4783.
22. **Higgins, R. R., H. J. Lucko, and A. Becker.** 1988. Mechanism of *cos* DNA cleavage of bacteriophage lambda terminase—multiple roles of ATP. Cell **54:**765–775.
23. **Jimenez, J., A. Santisteban, J. M. Carazo, and J. L. Carrascosa.** 1986. Computer graphic display method for visualizing three-dimensional biological structures. Science **232:**1113–1115.
24. **Hwang, Y., and M. Feiss.** 1996. Mutations affecting the high affinity ATPase center of gpA, the large subunit of bacteriophage lambda terminase, inactive the endonuclease activity of terminase. J. Mol. Biol. **261:**524–535.
25. **Hwang, Y., C. E. Catalano, and M. Feiss.** 1996. Kinetic and mutational dissection of the two ATPase activities of terminase, the DNA packaging enzyme of bacteriophage Chi. Biochemistry **35:**2796–2803.
26. **Kochan, J., J. L. Carrascosa, and H. Murialdo.** 1984. Bacteriophage lambda preconnectors: purification and structure. J. Mol. Biol. **174:**433–447.
27. **Koonin, E. V., V. I. Senkevich, and V. I. Chernos.** 1993. Gene A32 product of vaccinia virus may be an ATPase involved in viral DNA packaging as indicated by sequence comparisons with other putative viral ATPases. Virus Genes **7:**89–94.
28. **Lee, C. S., and P. Guo.** 1994. A highly sensitive system for *in vitro* assembly of bacteriophage ϕ29 of *Bacillus subtilis*. Virology **202:**1039–1042.
29. **Lee, C. S., and P. Guo.** 1995. In vitro assembly of infectious virions of double-stranded DNA phage ϕ29 from cloned gene products and synthetic nucleic acids. J. Virol. **69:**5018–5023.
30. **Lee, C. S., and P. Guo.** 1995. Sequential interactions of structural proteins in phage ϕ29 procapsid assembly. J. Virol. **69:**5024–5032.
31. **Manne, V. S., V. B. Rao, and L. W. Black.** 1982. A bacteriophage T4 DNA packaging related DNA-dependent ATPase-endonuclease. J. Biol. Chem. **257:**13223–13232.
32. **Michaud, G., A. Zachary, B. Rao, and L. Black.** 1989. Membrane-associated assembly of a phage T4 DNA entrance vertex structure studied with expression vectors. J. Mol. Biol. **209:**667–681.
33. **Morita, M., M. Tasaka, and H. Fujisawa.** 1993. DNA packaging ATPase of bacteriophage T3. Virology **193:**748–752.
34. **Panuska, J. R., and D. A. Goldthwait.** 1980. A DNA dependent ATPase from T4-infected *E. coli*. Purification and properties of a 63,000-dalton enzyme and its conversion to a 22,000-dalton form. J. Biol. Chem. **255:**5208–5214.
35. **Reid, R. J. D., J. W. Bodley, and D. Anderson.** 1994. Characterization of the prohead-pRNA interaction of bacteriophage ϕ29. J. Biol. Chem. **269:**5157–5162.
36. **Rishovd, S., O. J. Marvik, E. Jacobson, and B. H. Lindqvist.** 1994. Bacteriophage P2 and P4 morphogenesis: identification and characterization of the portal protein. Virology **200:**744–751.
37. **Rubinchik, S., W. Parris, and M. Gold.** 1994. The *in vitro* ATPases of bacteriophage λ terminase and its large subunit gene product A. J. Biol. Chem. **269:**13586–13593.
38. **Serwer, P.** 1987. The mechanism for producing two symmetries at the head-tail junction of bacteriophages: a hypothesis. J. Theor. Biol. **127:**155–161.
39. **Thomas, Jr., C. A., K. Saigo, E. McLeod, and J. Ito.** 1979. The separation of DNA segments attached to proteins. Anal. Biochem. **93:**158–166.
40. **Tomka, M. A., and C. E. Catalano.** 1993. Kinetic characterization of the ATPase activity of the DNA packaging enzyme from bacteriophage 1. Biochemistry **32:**11992–11997.
41. **Trottier, M., and P. Guo.** 1997. Approaches to determine stoichiometry of viral assembly components. J. Virol. **71:**487–494.
42. **Trottier, M., C. L. Zhang, and P. Guo.** 1996. Complete inhibition of virion assembly in vivo with mutant pRNA essential for phage ϕ29 DNA packaging. J. Virol. **70:**55–61.
43. **Tsuprun, V., D. Anderson, and E. H. Egelman.** 1994. The bacteriophage ϕ29 head-tail connector shows 13-fold symmetry in both hexagonally packed arrays and as single particles. Biophys. J. **66:**2139–2150.
44. **Turnquist, S., M. Simon, E. Egelman, and D. Anderson.** 1992. Supercoiled DNA wraps around the bacteriophage ϕ29 head-tail connector. Proc. Natl. Acad. Sci. USA **89:**10479–10483.
45. **Valpuesta, J. M., H. Fujisawa, S. Marco, J. M. Carazo, and J. Carrascosa.** 1992. Three-dimensional structure of T3 connector purified from overexpressing bacteria. J. Mol. Biol. **224:**103–112.
46. **Wichitwechkarn, J., S. Bailey, J. W. Bodley, and D. Anderson.** 1989. Prohead RNA of bacteriophage ϕ29: size, stoichiometry and biological activity. Nucleic Acids Res. **17:**3459–3468.
47. **Young, M., S. Kuhl, and P. von Hippel.** 1994. Kinetic theory of ATP-driven translocases on one-dimensional polymer lattices. J. Mol. Biol. **235:**1436–1446.
48. **Zhang, C. L., C.-S. Lee, and P. Guo.** 1994. The proximate 5′ and 3′ ends of the 120-base viral RNA (pRNA) are crucial for the packaging of bacteriophage ϕ29 DNA. Virology **201:**77–85.
49. **Zhang, C. L., K. Garver, and P. Guo.** 1995. Inhibition of phage ϕ29 assembly by antisense oligonucleotides targeting viral pRNA essential for DNA packaging. Virology **211:**568–576.
50. **Zhang, C. L., T. Tellinghuisen, and P. Guo.** 1997. Use of circular permutation to assess six bulges and four loops of DNA-packaging pRNA of bacteriophage Ø29. RNA **3:**315–322.
51. **Zhang, C. L., T. Tellinghuisen, and P. Guo.** 1995. Confirmation of the helical structure of the 5′/3′ termini of the essential DNA packaging pRNA of ϕ29. RNA **1:**1041–1050.
52. **Zhang, C. L., M. Trottier, and P. X. Guo.** 1995. Circularly permuted viral pRNA active and specific in the packaging of bacteriophage ϕ29 DNA. Virology **207:**442–451.
53. **Zuker, M.** 1989. On finding all suboptimal foldings of an RNA molecule. Science **244:**48–52.